

# Effect of Sc substitution for Y on structural properties and hyperfine interactions in $Y_{1-x}Sc_xFe_2$ compounds

Mieczysław Budzyński,  
Jan Sarzyński,  
Marek Wiertel,  
Zbigniew Surowiec

**Abstract** Measurements of X-ray diffraction and Mössbauer effect were made on a series of  $Y_{1-x}Sc_xFe_2$  polycrystalline samples ( $x = 0.0, 0.2, 0.5, 0.7, 0.8, 1.0$ ). It was found that the system has the cubic  $MgCu_2$  structure except for  $x = 1.0$  where hexagonal  $MgZn_2$  structure type is stable. The lattice constant decreases with increasing  $x$ . The results of Mössbauer effect study at room temperature show that the easy axes of magnetization remain in the  $\langle 111 \rangle$  direction for the cubic samples and  $\langle 100 \rangle$  for the hexagonal one. Curie temperatures  $T_C$  were determined from temperature dependence of the hyperfine magnetic fields. The concentration dependence of the hyperfine fields and  $T_C$  show similar trends, exhibiting a maximum at  $x = 0.8$ . The magnetic and structural behaviour show that, in spite of being isoelectronic, the substitution of Y by Sc induces clear changes in the structural and magnetic properties of the compounds under investigation.

**Key words** hyperfine interactions • Mössbauer effect • quasibinary Laves phase •  $Y_{1-x}Sc_xFe_2$

## Introduction

Systems of the type  $(T_{1-x}T'_x)Fe_2$  (where  $T = Y, Nb, Ti$ ;  $T' = Sc, Zr$ ) have been extensively investigated [3, 6, 8]. The main interest in these compounds is to understand their wide and complex magnetic behaviour. In the cubic C15  $YFe_2$  phase ( $MgCu_2$ , space group  $Fd\bar{3}m$ ) Fe atoms create regular tetrahedrons (16d positions) connected via their corners. Six Fe and six Y (8a positions) atoms surround each Fe atom composing its nearest neighbourhood (see Fig. 1a). In the hexagonal C14  $ScFe_2$  phase ( $MgZn_2$ , space group  $P6_3/mmc$ ) Fe atoms create a sublattice of regular tetrahedrons linked alternately by apexes (2a positions) or by their bases (6h positions). In this structure the population ratio of 6h and 2a sites is 3:1 (see Fig. 1b).

The compound  $YFe_2$  is a ferrimagnet ( $T_C = 542$  K) with a saturation magnetization of  $2.9 \mu_B$  per formula unit [4]. More detailed theoretical [7] and experimental neutron diffraction investigations [11] have been shown that all Fe atoms have a magnetic moment of about  $1.66(8) \mu_B$  and an antiparallel induced magnetic moment at Y sites of about  $-0.45(4) \mu_B$  exists. This moment is a result of hybridization of  $3d$  Fe and  $4d$  Y bands [7]. The Laves phase  $ScFe_2$  is a ferrimagnet ( $T_C = 542(9)$  K) in which at 4.2 K all Fe atoms have a magnetic moment of about  $1.37 \mu_B$  [5]. Magnetic moments of  $1.54(1.60) \mu_B$  for Fe in  $ScFe_2$  on the 2a (6h) sites were obtained from calculations by means of the local spin density approximation [1]. Sc atoms have a magnetic moment of  $0.52 \mu_B$  in the opposite direction to Fe moments [10].

In the C15 structure, all Fe atoms have local  $\bar{3}m$  symmetry with a threefold axis in the  $\langle 111 \rangle$  direction and the electric field gradient EFG is axially symmetric about this axis. For the pure  $YFe_2$  intermetallic an easy axis of magnetization has the same direction. In the magnetically ordered state,

M. Budzyński, J. Sarzyński, M. Wiertel, Z. Surowiec✉  
Institute of Physics,  
M. Curie-Skłodowska University,  
1 M. Curie-Skłodowska Sq., 20-031 Lublin, Poland,  
Tel.: +48 81/ 537 62 20, Fax: +48 81/537 61 91,  
e-mail: zsurowie@tytan.umcs.lublin.pl

Received: 17 July 2002, Accepted: 15 November 2002

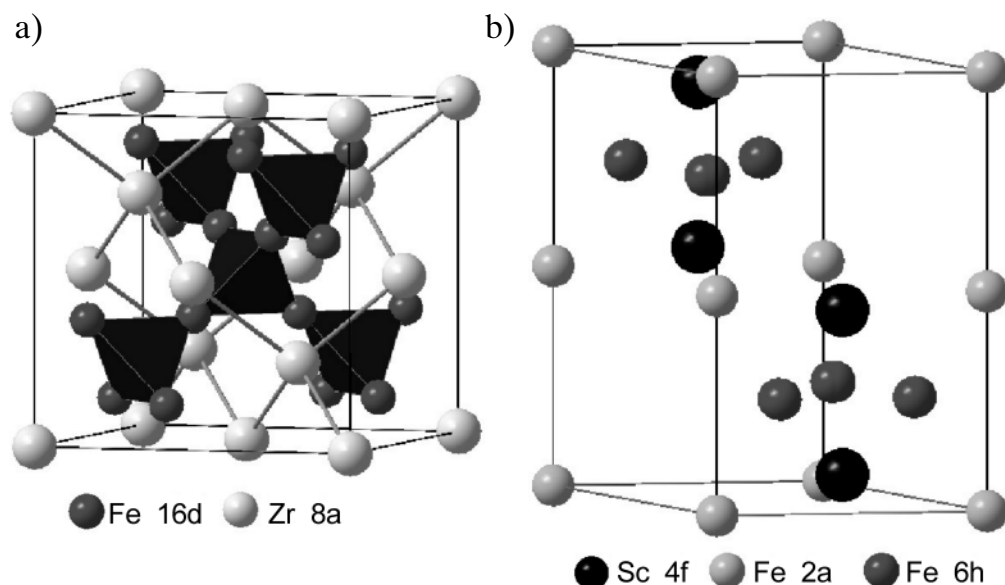


**Fig. 1.** Crystallographic structures of a)  $\text{YFe}_2$  C15 and b)  $\text{ScFe}_2$  C14 Laves phases.

local magnetic field makes two possible angles:  $70^\circ 32'$  and  $0^\circ$  with the principal axis of the EFG. This determines two distinct types of magnetically non-equivalent Fe positions called I and II, respectively, with a population ratio of 3:1. In the C14 lattice the principal axes of the local EFGs for 6h sites are perpendicular to the  $c$ -axis being simultaneously an easy axis of magnetization. In the case of 2a sites, the relevant axes overlap. This fact is reflected in the Mössbauer spectra through the observed different values of quadrupole shifts  $\varepsilon_Q = QS(3 \cos^2 \theta - 1)/2$ .

The purpose of our study is to examine the effect of Sc substitution for Y on structural properties and hyperfine interactions in  $\text{Y}_{1-x}\text{Sc}_x\text{Fe}_2$  compounds.

## Experimental

Intermetallic compounds of  $\text{Y}_{1-x}\text{Sc}_x\text{Fe}_2$  ( $x = 0.0, 0.2, 0.5, 0.7, 0.8, 1.0$ ) were prepared by arc melting of the raw

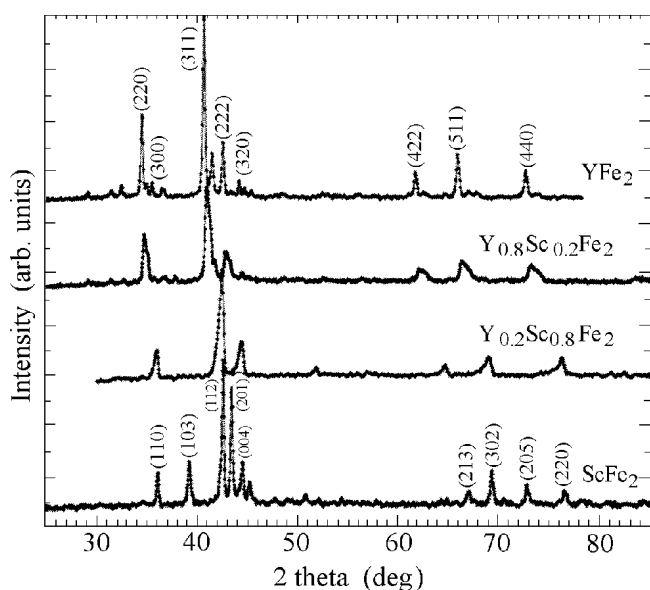


**Fig. 2.** XRD patterns of  $\text{Y}_{1-x}\text{Sc}_x\text{Fe}_2$  for  $x = 0, 0.2, 0.8$  and  $1.0$  from the top to bottom, respectively.

materials of 99.9% purity under an inert argon atmosphere. The ingots were annealed in vacuum at about 1073 K for one week to ensure their homogeneity. Phase analysis was carried out by means of X-ray powder diffraction with  $\text{CuK}\alpha$  radiation. The scans were realized in the range of  $24^\circ$  to  $90^\circ$  ( $2\theta$ ). Mössbauer spectra of powder samples were recorded using a constant acceleration spectrometer in the 300 to 800 K temperature range with a  $^{57}\text{Co}(\text{Rh})$  source. The data of the Mössbauer spectra were fitted using a least-squares fitting, where the quadrupole interaction is treated as a perturbation to the hyperfine field. The isomer shift values are given relative to  $\alpha$ -Fe at room temperature.

## Results and discussion

The X-ray diffraction patterns representative of  $\text{Y}_{1-x}\text{Sc}_x\text{Fe}_2$  series are shown in Fig. 2 and indicate that the compounds for  $x < 1.0$  crystallize in the cubic C15 structure and  $\text{ScFe}_2$  in the hexagonal C14 structure. However, a residual amount of some unidentified phases was detected in the patterns for  $\text{YFe}_2$  and  $\text{ScFe}_2$  in particular. On the other hand, their presence is not disclosed in the Mössbauer results.

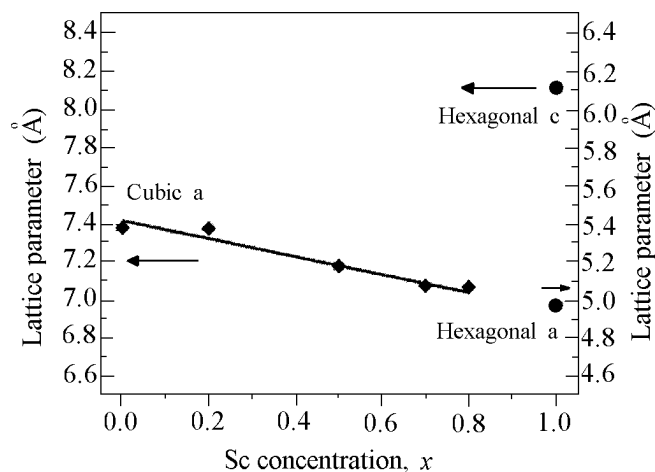


**Fig. 3.** The lattice constant values vs. the Sc concentration  $x$  in the  $\text{Y}_{1-x}\text{Sc}_x\text{Fe}_2$  phases from XRD.

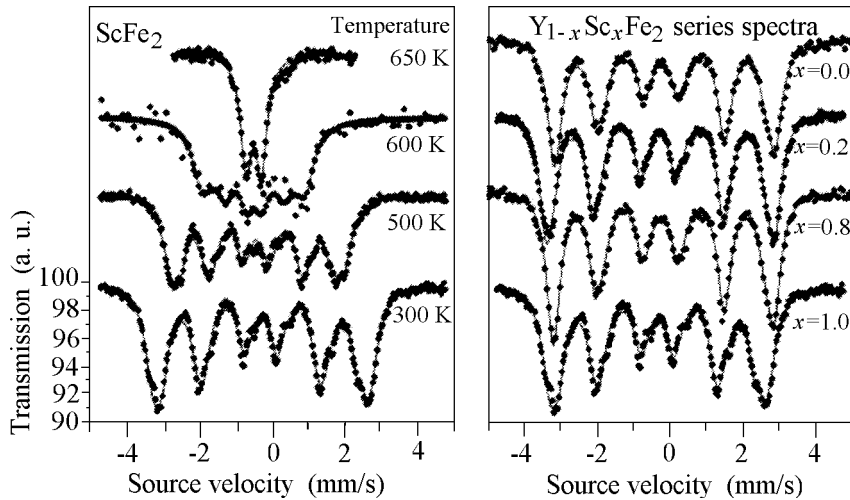


**Fig. 4.**  $^{57}Fe$  Mössbauer spectra of  $ScFe_2$  at various temperatures (left) and spectra of  $Y_{1-x}Zr_xFe_2$  for  $x = 0, 0.2, 0.8$  and  $1.0$  at room temperature (right).

Figure 3 presents the lattice parameters as a function of the Sc concentration for both types of crystal structures observed. The replacement of bigger Y atoms by smaller Sc in the C15 phase atoms leads to the decrease of lattice constant  $a$  according to the Vegard's law.

Figure 4 shows typical Mössbauer spectra of  $ScFe_2$  measured at various temperatures and spectra of  $Y_{1-x}Zr_xFe_2$  for  $x = 0, 0.2, 0.8, 1.0$  recorded at room temperature.

The results obtained for the hyperfine interaction parameters at room temperature are given in Figs. 5 and 6. From the composition dependence of hyperfine magnetic fields (HMF) shown in Fig. 5a it can be seen that a maximum occurs at about  $x = 0.8$ . A similar change in the HMF was also observed in a study of  $Y_{1-x}Zr_xFe_2$  [6]. The difference of values  $B_I$  and  $B_{II}$  related to the respective sites in the  $YFe_2$  can be fully explained by different dipole contributions [2]. This difference decreases with increasing concentration  $x$  in the quasibinary samples. In the hexagonal  $ScFe_2$  phase hyperfine fields for both 6h and 2a crystallographic positions are equal. The quadrupole shift  $\epsilon_{QII}$  for  $\theta = 0^\circ$  should be equal to  $-3$  times  $\epsilon_{QI}$  for  $\theta = 70^\circ 32'$  in the cubic samples. The observed values exhibit the difference in sign in compliance with the above relation but they are in an improper ratio of about  $-2:1$  (see Fig. 5b). Therefore, it is concluded that the direction of HMF somewhat differs

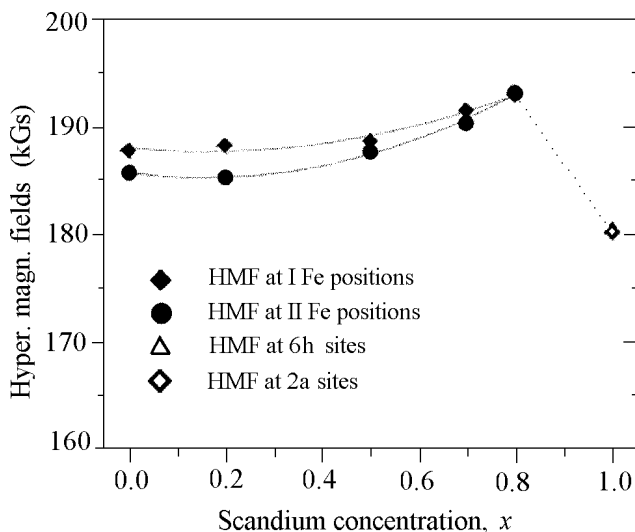
from the  $\langle 111 \rangle$  direction in the cubic compounds  $Y_{1-x}Sc_xFe_2$ .

The quadrupole shift values for both components exhibit insignificant temperature dependence. They decrease by about 4%/100 K in the whole temperature range.

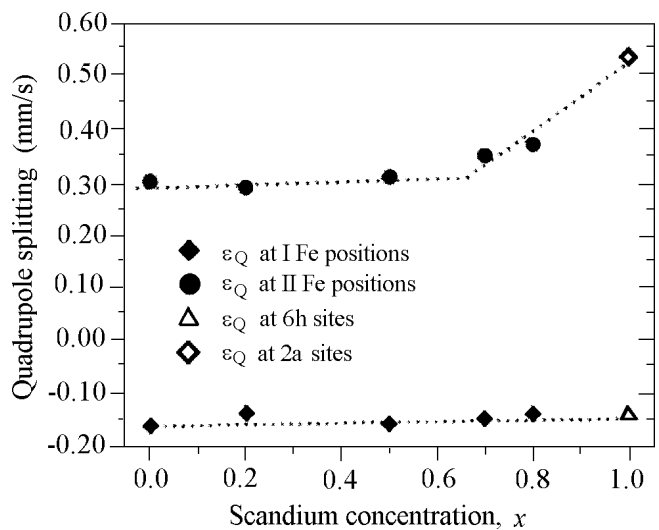
The thermal evolution of the magnetic hyperfine field  $H$  derived from numerical analysis is shown in Fig. 6 together with the Brillouin curve fitted to the experimental points. Extrapolation of this curve to the zero field leads to the determination of Curie temperature. For the pure binary phase  $YFe_2$  (Fig. 6a)  $T_C = 527$  K, is in reasonable agreement with the result of reference [4]. The highest  $T_C$  (685 K) is achieved in the case of  $Y_{0.2}Sc_{0.8}Fe_2$  (Fig. 6b).

Figure 7 shows the variation of the Curie temperature with the scandium concentration for  $Y_{1-x}Sc_xFe_2$  alloys as determined by the extrapolated Brillouin curve to zero fields. As can be seen the  $T_C$  increases almost linearly with  $x$  with a coefficient of about 5.85 K/at.% Sc in the concentration range from 0 to 0.8 and decreases for  $x > 0.8$ .

A strong influence of the replacement of Y atoms with Sc atoms on the magnetic and crystallographic properties of the discussed compounds is surprising if we set our results for the concentration dependence of HMF and  $T_C$  against the fact that Sc 4d and Y 3d atoms have the same number of valence electrons. The main contribution to the hyperfine magnetic field on Fe results from net polarization of



**Fig. 5a.** The hyperfine magnetic field values vs. the Sc concentration  $x$  in  $Y_{1-x}Sc_xFe_2$  at room temperature.



**Fig. 5b.** The quadrupole shift  $\epsilon_Q$  values vs. the Sc concentration  $x$  in  $Y_{1-x}Sc_xFe_2$  at room temperature.

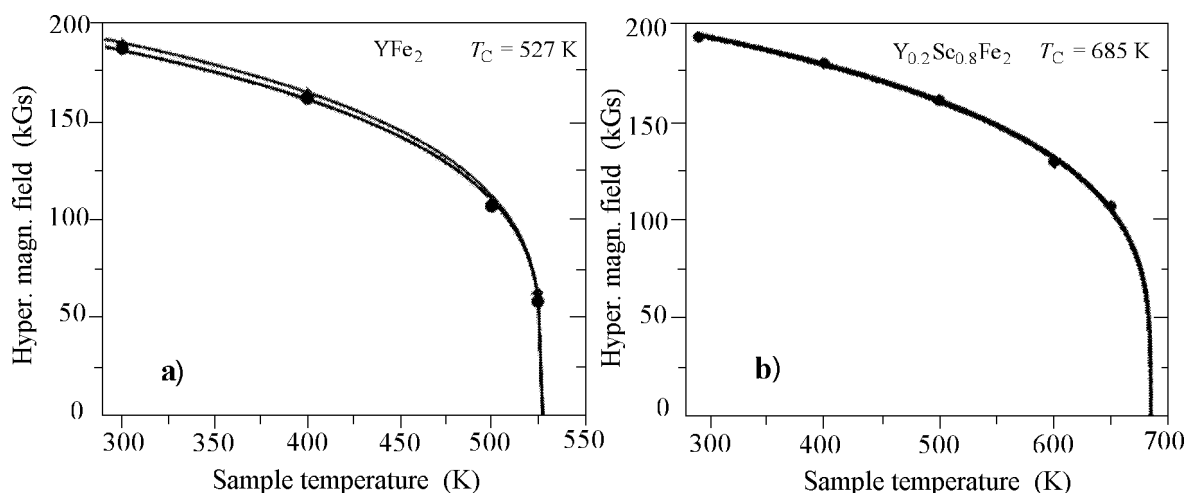


**Fig. 6.** Temperature dependence of the magnetic hyperfine fields derived from the computer fits to the  $^{57}\text{Fe}$  Mössbauer spectra obtained for the a)  $\text{YFe}_2$ , b)  $\text{Y}_{0.2}\text{Sc}_{0.8}\text{Fe}_2$ . The continuous line represents the least-squares fit of the Brillouin function.

the inner  $s$ -type electrons by its own magnetic moment. The contribution is proportional to this moment. Hence our result for the concentration dependence of HMF suggests that magnetic moment of Fe atom increases in the range of concentration  $x$  smaller than 0.8, contrary to the theoretical predictions [1]. The increase of magnetic moments takes place only for  $x$  larger than about 0.8.

The isomer shift values are almost identical for both types of Fe sites and, therefore, only dependence on  $x$  and  $T$  for averaged values of them is shown in Fig. 8. They change linearly with increasing sample temperature and become more negative. This tendency holds above the Curie temperature. Such temperature dependence is caused by the second-order Doppler shift.

The IS value changes almost monotonically with  $x$  from  $-0.09$  mm/s for pure  $\text{YFe}_2$  to  $\text{IS} = -0.19$  mm/s for pure  $\text{ScFe}_2$  at room temperature. In the case of  $^{57}\text{Fe}$  probe this means that the  $s$  electron density on the nucleus increases. The possible explanations of this concentration dependence are as follows. Firstly, the density of the  $4s$  conduction electrons may increase directly due to the decrease of the

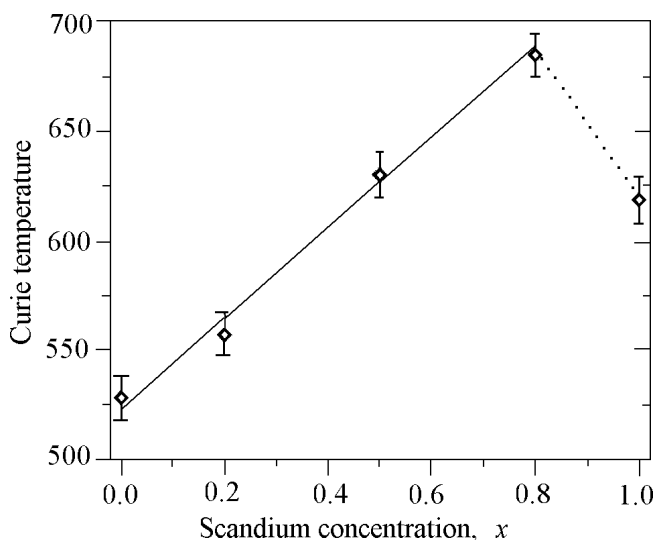


**Fig. 7.** The variation of the Curie temperature  $T_C$  values with Sc concentration determined by extrapolation of the Brillouin curve to the zero fields.

nearest neighbour distances (from  $2.61 \text{ \AA}$  in  $\text{YFe}_2$  to  $2.48 \text{ \AA}$  in  $\text{ScFe}_2$ ). Secondly, the density of the inner  $3s$  Fe electrons may increase as a result of the weaker shielding of these electrons by the  $3d$  Fe electrons. It is known [1] that when  $4d$  transition atoms  $A$  are substituted by  $3d$  atoms in the quaternary Laves  $\text{AFe}_2$  compound, hybridization between the  $3d$  Fe bands and the  $d$  bands of the  $A$  atom becomes stronger. Then, the width of the Fe  $3d$  band becomes larger and the degree of the localization of states in such a band decreases. In this situation a screening of  $3s$  Fe electrons by the  $3d$  Fe electrons becomes weaker and the density of  $s$  electrons at the nucleus increases. Then, an absolute value of the isomer shift reaches its maximum.

## Summary

The substitution of the Sc atoms for the Y atoms in the polycrystalline  $\text{Y}_{1-x}\text{Sc}_x\text{Fe}_2$  alloys leads to an increase of the

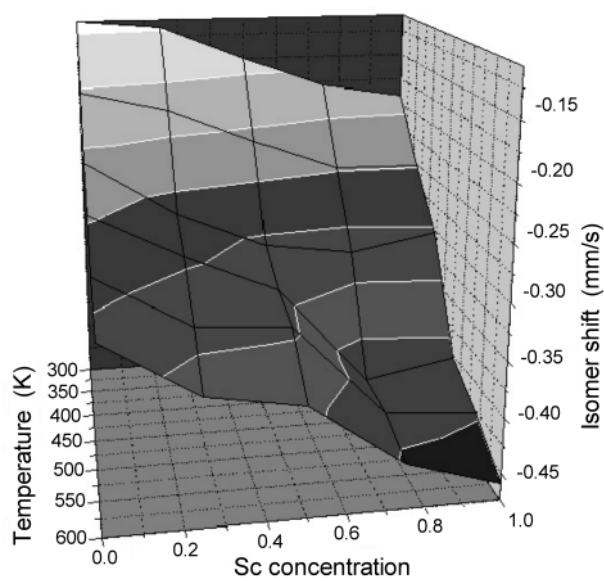


**Fig. 8.** The distribution of the values of the isomer shift (IS) vs. the concentration Sc and the temperature in  $\text{Y}_{1-x}\text{Sc}_x\text{Fe}_2$ , with respect to  $\alpha\text{-Fe}$ . For explanations see text.

hyperfine magnetic field and the Curie temperature in the cubic crystalline phase and the decrease of these quantities in the hexagonal crystalline phase. From the investigations for analogous quasibinary alloys [9] it is known that the structural phase transition takes place for the concentration  $x$  equal about to 0.8–0.9. On the basis of our results we could find some discrepancies between the experimental and theoretical predictions for the changes of the Fe magnetic moments versus the concentration  $x$  in the quasibinary intermetallic compounds. The increase of the absolute value of the isomer shift in the  $Y_{1-x}Sc_xFe_2$  phases with increasing temperature can be fully explained on the basis of the second-order Doppler shift. The increase of  $s$  electron density at Fe nuclei in the quasibinary  $Y_{1-x}Sc_xFe_2$  samples, which manifests itself in the increase of the isomer shift, too, may result from changes in the Fe band structure. The replacement of Sc atoms by the Y ones leads to a larger extent of delocalization of  $3d$  Fe electrons charge and hence to the weaker shielding of  $3s$  Fe electrons.

## References

1. Asano S, Ishida S (1988) Magnetism and crystal structure of Laves phase compounds. *J Phys F* 18:501–515
2. Bowden GJ, Bunbury DSP, Guimaraes AP, Snyder RE (1968) Mössbauer studies of the cubic Laves iron-rare-earth intermetallic compounds. *J Phys C* 1:1376–1387
3. Budzyński M, Sarzyński J, Surowiec Z, Wiertel M (2001) Mössbauer and X-ray diffraction studies of  $Zr_{1-x}Ti_xFe_2$  Laves phase compounds. *Acta Phys Pol A* 100:717–722
4. Buschow KHJ, van Staple RP (1970) Magnetic properties of some cubic rare-earth-iron compounds of the type  $RFe_2$  and  $R_xY_{1-x}Fe_2$ . *J Appl Phys* 41:4066–4069
5. Ikeda K, Takuro N, Yamada T, Yamamoto M (1974) Ferromagnetism in  $Fe_2Sc$  with hexagonal  $MgZn_2$ -type structure. *J Phys Soc Jpn* 36:611–611
6. Itoh K, Kanenematsu K, Kobashi K (1989) Mössbauer study of  $Y_{1-x}Zr_xFe_2$ . *J Phys Soc Jpn* 58:4650–4651
7. Mohn P, Schwarz K (1985) Binding mechanism and itinerant magnetism of  $ZrFe_2$  and  $YFe_2$ . *Physica B* 130:26–28
8. Nishihara Y, Yamaguchi Y (1985) Magnetic structures in the  $Sc_{1-x}Ti_xFe_2$  system – magnetic phase transitions in itinerant electron systems. *J Phys Soc Jpn* 54:1122–1130
9. Pokatilov VS, Golikova VV (1990) Hyperfine fields at  $^{45}Sc$  and  $^{89}Y$  nuclei in Laves intermetallic compounds  $Sc_{1-x}Y_xFe_2$  with cubic structure. *Izv Akad Nauk SSSR, Fizika* 54:1736–1738 (in Russian)
10. Pösinger A, Steiner W (1991) High field Mössbauer investigations of the magnetic phase transition in  $Sc_{0.25}Ti_{0.75}Fe_2$  at 4.2 K. *J Magn Magn Matter* 98:19–24
11. Ritter C (1989) Polarised neutron study of the magnetic ordering in the simple alloy  $YFe_2$ . *J Phys-Condens Matter* 1:2765–2769